RAPID COMMUNICATIONS IN MASS SPECTROMETRY
Rapid Commun. Mass Spectrom. 2010; **24**: 1770–1778
Published online in Wiley InterScience (www.interscience.wiley.com) DOI: 10.1002/rcm.4579

RCM

Structural identification of mouse urinary metabolites of pterostilbene using liquid chromatography/tandem mass spectrometry

Xi Shao[1,2,3,4], Xiaoxin Chen[5], Vladimir Badmaev[6], Chi-Tang Ho[4] and Shengmin Sang[1,2,3]*

[1]Center for Excellence in Post-Harvest Technologies, North Carolina Agricultural and Technical State University, North Carolina Research Campus, 500 Laureate Way, Kannapolis, NC 28081, USA
[2]Human Nutrition Research Program, Julius L. Chambers Biomedical/Biotechnology Research Institute, North Carolina Central University; North Carolina Research Campus, 500 Laureate Way, Kannapolis, NC 28081, USA
[3]Food Science Graduate Program, Rutgers University, 65 Dudley Road, New Brunswick, NJ 08901, USA
[4]Department of Food Science, Rutgers University, 65 Dudley Road, New Brunswick, NJ 08901, USA
[5]Cancer Research Program, Julius L. Chambers Biomedical/Biotechnology Research Institute, North Carolina Central University, 700 George Street, Durham, NC 27707, USA
[6]Laboratory of Applied Pharmacology, 1440-6 Forest Hill Road, Staten Island, NY 10314, USA

Received 8 January 2010; Revised 11 April 2010; Accepted 14 April 2010

Pterostilbene, the dimethoxy derivative of resveratrol, has drawn much attention recently due to its potential beneficial health effects. The metabolic fate of pterostilbene, however, is not well understood. In the present study, we identified nine novel mouse urinary pterostilbene metabolites, pterostilbene glucuronide, pterostilbene sulfate, mono-demethylated pterostilbene glucuronide, mono-demethylated pterostilbene sulfate, mono-hydroxylated pterostilbene, mono-hydroxylated pterostilbene glucuronide, mono-hydroxylated pterostilbene sulfate, and mono-hydroxylated pterostilbene glucuronide sulfate, using liquid chromatography/atmospheric pressure chemical ionization and electrospray ionization tandem mass spectrometry. The structures of these metabolites were confirmed by analyzing the MS^n (n = 1–3) spectra. To our knowledge, this is the first report of the identification of urinary metabolites of pterostilbene in mice. Copyright © 2010 John Wiley & Sons, Ltd.

Pterostilbene is a naturally occurring stilbenoid compound originated from several natural plant sources including deerberries, blueberries, as well as some plants widely used in traditional medicine, such as *Pterocarpus marsupium*, *Pterocarpus santalinm*, and *Vitis vinifera* leaves.[1–3] As a dimethyl ether analogue of resveratrol, pterostilbene has drawn much attention recently due to its potential health benefits as an antioxidant, anticancer, antidiabetic and antihypolipidemic agent.[4–9] It has been reported that the peroxyl-radical scavenging activity of pterostilbene is the same as that of resveratrol.[8] Suh *et al*. found that administration of 40 ppm of pterostilbene for 8 weeks significantly suppressed azoxymethane-induced formation of aberrant crypt foci (ACF) (57% inhibition, $P < 0.001$) and multiple clusters of aberrant crypts (29% inhibition, $P < 0.01$).[6] Dietary pterostilbene also suppressed azoxymethane-induced colonic cell proliferation and iNOS expression.[6] Cichocki *et al*. reported that pterostilbene is equally potent as resveratrol in inhibiting 12-*O*-tetradecanoylphorbol-13-acetate activated NFkappaB, AP-1, COX-2, and iNOS in mouse epidermis.[5] In addition, pterostilbene has been reported to significantly lower the blood glucose level in hyperglycemic rats.[7–9]

**Correspondence to*: S. Sang, Center for Excellence in Post-Harvest Technologies, North Carolina Agricultural and Technical State University, North Carolina Research Campus, 500 Laureate Way, Kannapolis, NC 28081, USA.
E-mail: ssang@ncat.edu

Due to the various potential health benefits of pterostilbene, a good understanding of its metabolic fate is crucial. However, only one study has reported that glucuronidated pterostilbene is the major metabolite in rat liver microsomes; no tandem mass spectrum is provided in this study to further confirm the structure of glucuronidated pterostilbene.[10] There have been no reports on the biotransformation of pterostilbene in mice. In recent years, liquid chromatography/tandem mass spectrometry (LC/MS/MS) has evolved as a valuable tool for structural analysis of the metabolites of many bioactive polyphenols. The use of ion traps in metabolite identification takes advantage of the high sensitivity and multiple stage MS/MS (MS^n) capabilities of this kind of instrument. In the present study, we analyzed the mouse urinary metabolic profile of pterostilbene using liquid chromatography/atmospheric pressure chemical ionization (APCI) and electrospray ionization (ESI) tandem mass spectrometry. The structures of nine major metabolites were identified by analyzing the MS^2 and MS^3 spectra of each compound.

EXPERIMENTAL

Materials

Pterostilbene was provided by Sarbinsa Corporation (Piscataway, NJ, USA). LC/MS-grade solvents and other reagents were obtained from Fisher Scientific (Pittsburgh, PA, USA).

HPLC-grade water was prepared using a Millipore Milli-Q purification system (Bedford, MA, USA). Sulfatase from *Aerobacter aerogenes* and β-glucuronidase from *Helix aspersa* were obtained from Sigma (St. Louis, MN, USA).

Treatment of mice and urine collection

Experiments with mice were carried out according to a protocol approved by the Institutional Review Board for the Animal Care and Facilities Committee (IACUC No. SS1 08-08-2008) at North Carolina Central University. Female C57BL/6J mice (24–30 g) were purchased from the Jackson Laboratory (Bar Harbor, ME, USA) and allowed to acclimate for at least 1 week prior to the start of the experiment. The mice were housed 5 per cage for each group and maintained in air-conditioned quarters with a room temperature of $20 \pm 2^{\circ}C$, relative humidity of $50 \pm 10\%$, and an alternating 12-h light/dark cycle. Mice were fed Purina Rodent Chow #5001 (Research Diets) and water, and were allowed to eat and drink *ad libitum*. Pterostilbene in dimethyl sulfoxide (DMSO) was administered to mice by oral gavage (200 mg/kg), and urine samples were collected in metabolism cages (5 mice per case) for 24 h after administration of vehicle (control group, $n = 5$) or pterostilbene (treated group, $n = 5$). These samples were stored at $-80^{\circ}C$ before analysis.

Urine sample preparation

For the metabolic profile, urine samples (50 μL from each group, control group and pterostilbene-treated group) were added to 950 μL methanol to precipitate proteins. After centrifugation at 17×1000 rpm for 5 min, the supernatant was transferred into vials for LC/MS analysis. Enzymatic deconjugation was performed as described previously with slight modification.[11] In brief, duplicate samples were prepared in the presence of β-glucuronidase (250 U) and sulfatase (3 U) for 24 h at 37°C and then extracted twice with ethyl acetate. The ethyl acetate fraction was dried under vacuum, and the solid was resuspended in 200 μL of 80% aqueous methanol with 0.1% acetic acid for further LC/MS analysis.

LC/PDA/APCI/ESI-MS method

LC/PDA/MS analysis was carried out with a Thermo-Finnigan Spectra System which consisted of an Accela high-speed MS pump, an Accela refrigerated autosampler, an Accela photodiode array (PDA) detector, and an LCQ Fleet ion trap mass detector (Thermo Electron, San Jose, CA, USA) incorporated with atmospheric pressure chemical ionization (APCI) and electrospray ionization (ESI) interfaces. A Luna C18 column (50×2.0 mm i.d., 3 μm; Phenomenex, Torrance, CA, USA) was used for separation at a flow rate of 0.3 mL/min. The column was eluted with 100% solvent A (5% aqueous methanol with 0.2% acetic acid) for 5 min, followed by linear increases in B (95% aqueous methanol with 0.2% acetic acid) to 50% from 5 to 10 min, to 65% from 10 to 25 min, to 100% from 25 to 40 min, and then with 100% B from 40 to 45 min. The column was then re-equilibrated with 100% A for 5 min. The LC eluent was introduced into the APCI or ESI interface. The positive ion polarity mode was set for the APCI

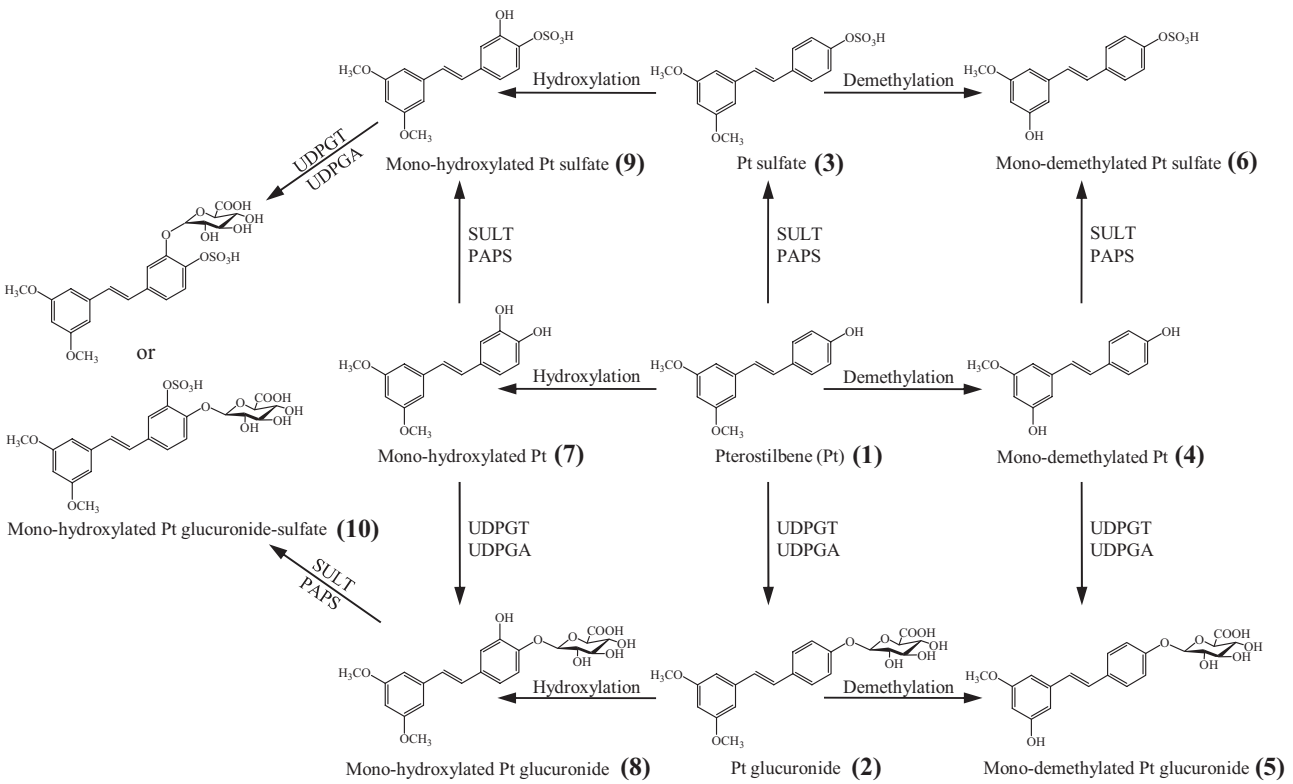

Figure 1. Structures of pterostilbene and its major metabolites and possible biotransformation pathways of pterostilbene. SULT: sulfotransferase; PAPS: adenosine 3′-phosphate 5′-phosphosulfate (sulfuryl group donor); UDPGT: uridine diphosphate glucuronosyltransferase; UDPGA: uridine diphosphate glucuronic acid.

DOI: 10.1002/rcm

source and nitrogen gas was used as the sheath gas and auxiliary gas. Optimized source parameters include APCI capillary temperature (280°C), APCI vaporizer temperature (325°C), capillary voltage (43 V), sheath gas flow rate (20 units), auxiliary gas flow rate (5 units), and tube lens (115 V). These parameters were tuned using authentic pterostilbene.

The negative ion polarity mode was set for the ESI source with the voltage on the ESI interface maintained at approximately 5 kV. Nitrogen gas was used as the sheath gas and auxiliary gas. Optimized source parameters include ESI capillary temperature (300°C), capillary voltage (–50 V), ion spray voltage (3.6 kV), sheath gas flow rate (30 units), auxiliary gas flow rate (5 units), and tube lens (–124.65 V). These parameters were tuned using authentic pterostilbene. The collision-induced dissociation (CID) for both APCI and ESI was conducted with an isolation width of 2 Da and normalized collision energy of 35 for MS^2 and MS^3. Default automated gain control target ion values were used for MS, MS^2, and MS^3 analyses. The wavelength of the PDA-UV detector was set at 280 nm. Data acquisition was performed with Xcalibur version 2.0 (Thermo Electron, San Jose, CA, USA).

RESULTS AND DISCUSSION

The strategy that we used for structural characterization of pterostilbene metabolites was knowledge-based metabolic identification. It has been reported that resveratrol is a good substrate for phase II biotransformation, such as glucuronidation (M + 176) and sulfation (M + 80).[12] Since pterostilbene has one free hydroxyl group, we predict that pterostilbene is also a substrate for glucuronidation and sulfation. In our previous study on the biotransformation of polymethoxyflavones, we found that demethylation (M–14) was the major biotransformation pathway for nobiletin, one of the major polymethoxyflavones in orange peels.[13] Therefore, we predict that demethylation will also be the major biotransformation pathway for pterostilbene. In addition, it has been reported that resveratrol can be metabolized to form hydroxylated metabolites, such as piceatannol, and glutathione conjugates under *in vitro* conditions.[14] We used selected-ion monitoring (SIM) mode to search all the possible pterostilbene metabolites from mouse urine samples collected after administration of pterostilbene (200 mg/kg, *i.g.*). Those metabolites included pterostilbene glucuronide (*m/z*

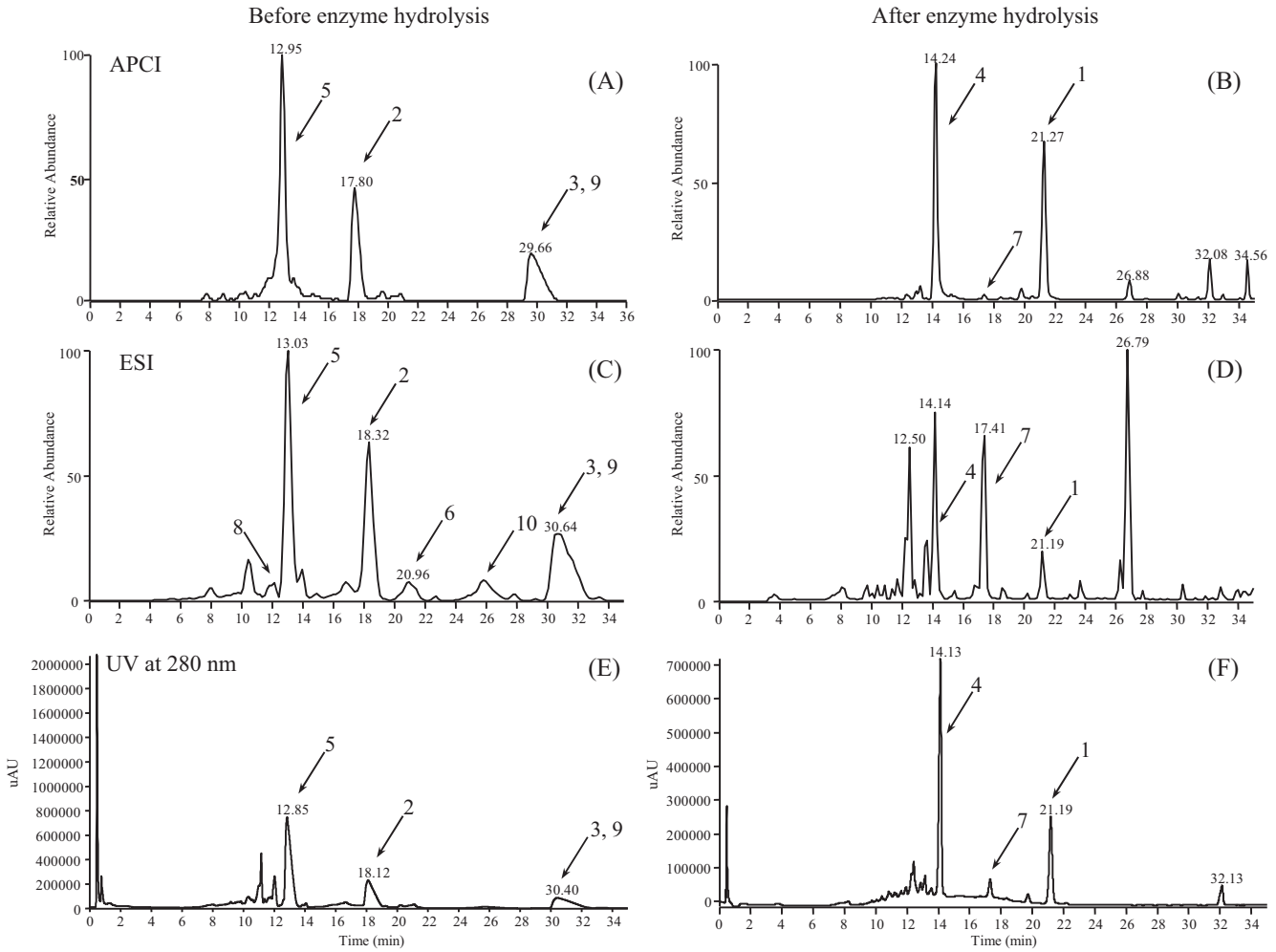

Figure 2. LC chromatograms of urine samples collected from pterostilbene-treated mice obtained using the positive APCI-MS interface: (A) before and (B) after enzymatic hydrolysis; by negative ESI-MS interface: (C) before and (D) after enzymatic hydrolysis; and by PDA-UV detector (280 nm): (E) before and (F) after enzymatic hydrolysis.

DOI: 10.1002/rcm

Table 1. Major mouse urinary metabolites of pterostilbene

Compound/metabolite name	Peak #	Retention time (min)
Pterostilbene (Pt)	1	21.27
Pt glucuronide	2	17.80
Pt sulfate	3	30.64
Mono-demethylated Pt	4	14.24
Mono-demethylated Pt glucuronide	5	12.95
Mono-demethylated Pt sulfate	6	20.96
Mono-hydroxylated Pt	7	17.41
Mono-hydroxylated Pt glucuronide	8	12.32
Mono-hydroxylated Pt sulfate	9	30.64
Mono-hydroxylated Pt glucuronide sulfate	10	27.49

432), pterostilbene sulfate (*m*/*z* 336), pterostilbene glutathione conjugate (*m*/*z* 561), pterostiblene cysteine conjugate (*m*/*z* 375), mono-demethylated pterostilbene (*m*/*z* 242), mono-demethylated pterostilbene mono-glucuronide (*m*/*z* 418), mono-demethylated pterostilbene mono-sulfate (*m*/*z* 322), mono-demethylated pterostilbene mono-glucuronide and mono-sulfate (*m*/*z* 498), mono-demethylated pterostilbene di-glucuronide (*m*/*z* 594), mono-demethylated pterostilbene di-sulfate (*m*/*z* 402), resveratrol (*m*/*z* 228) and its reported mono-glucuronide (*m*/*z* 404) and mono-sulfate (*m*/*z* 308), and hydroxylated pterostilbene (*m*/*z* 272) and its related mono-glucuronide (*m*/*z* 448), mono-sulfate (*m*/*z* 352), and glucuronide sulfate (*m*/*z* 528) metabolites.

We analyzed the urine samples collected both from control mice and mice treated with 200 mg/kg pterostilbene through oral gavage using positive APCI-MS, negative ESI-MS, and UV (280 nm) detection (Figs 1 and 2 and Supplementary Fig. S1, see Supporting Information). Among all the possible metabolites that we searched, we identified pterostilbene glucuronide, pterostilbene sulfate, mono-demethylated pterostilbene, mono-demethylated pterostilbene glucuronide, mono-demethylated pterostilbene sulfate, mono-hydroxylated pterostilbene, mono-hydroxylated pterostilbene glucuronide, mono-hydroxylated pterostilbene sulfate, and mono-hydroxylated pterostilbene glucuronide sulfate as the urinary metabolites of pterostilbene in mice (Figs. 1 and 2 and Table 1). This indicates that glucuronidation, sulfation, demethylation, and hydroxylation are the major biotransformation pathways of pterostilbene in mice. We found that APCI-MS detection was more sensitive to free pterostilbene and its mono-demethylated metabolite than ESI-MS detection (Fig. 2). This may be due to the fact that APCI-MS is more sensitive to less polar compounds, such as pterostilbene and mono-demethylated pterostilbene, than ESI-MS. We could only detect the molecular ions of the sulfate metabolites with ESI-MS detection because ESI is a softer ionization process than APCI. The LC chromatograms obtained under UV

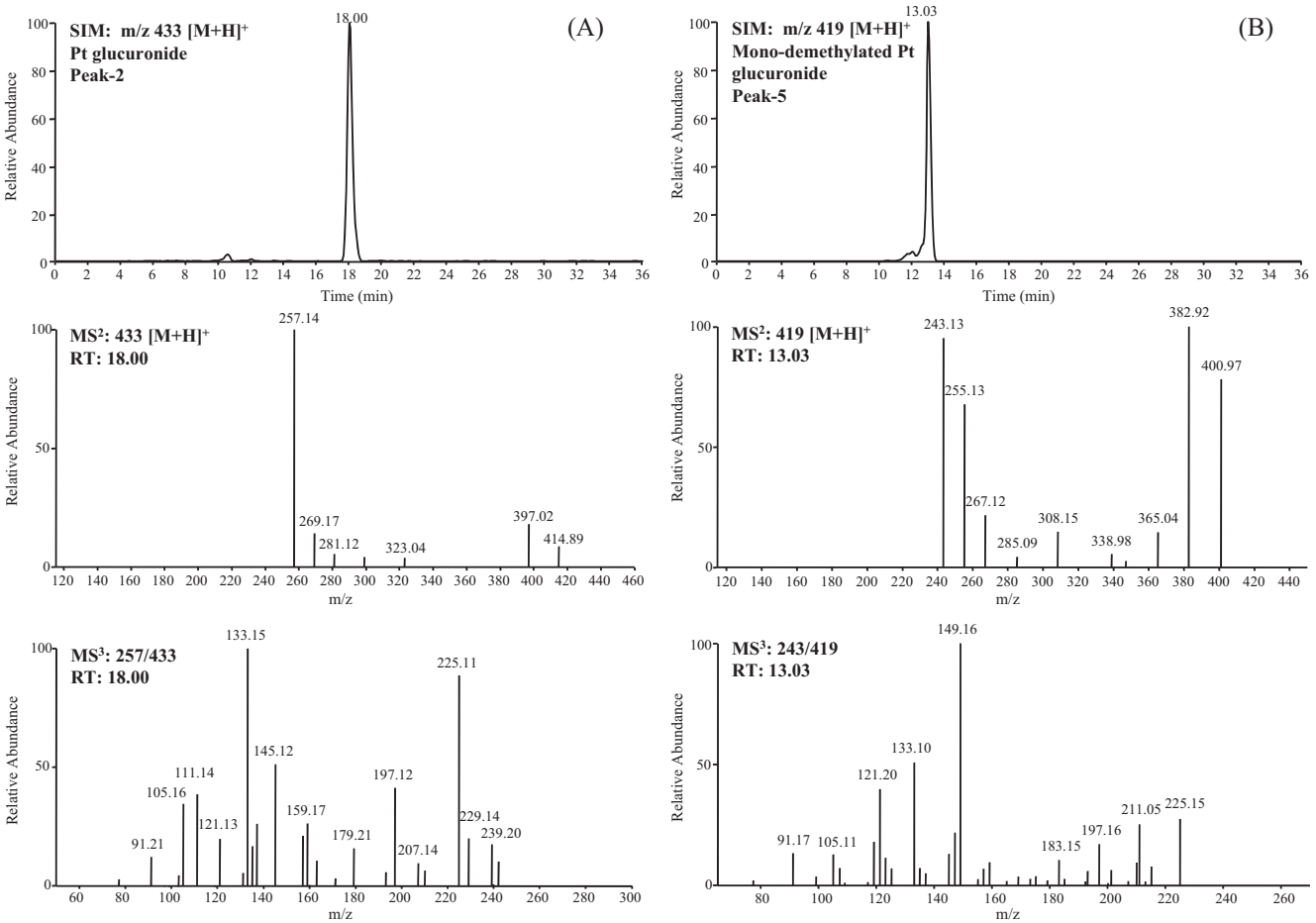

Figure 3. LC/APCI-MS^2 and -MS^3 (positive ion) spectra of (A) pterostilbene glucuronide (peak 2 in Fig. 2(A)) and (B) mono-demethylated pterostilbene glucuronide (peak 5 in Fig. 2(A)). Pt stands for pterostilbene.

DOI: 10.1002/rcm

detection (280 nm) were similar to those obtained under APCI-MS detection (Fig. 2).

Identification of the conjugated metabolites of pterostilbene

Mono-glucuronidated pterostilbene (2) and mono-sulfatated pterostilbene (3) were identified as the two conjugated metabolites of pterostilbene (1) using LC/APCI and LC/ESI tandem mass spectrometry (Figs. 1 and 2 and Table 1). We observed one major peak (peak 2 at 17.80 min) in the LC chromatogram obtained from APCI-MS detection (Fig. 2(A)) with the molecular ion m/z 433 $[M+H]^+$ (257 + 176) indicating that this peak was the glucuronide metabolite of pterostilbene. This was further confirmed by observing m/z 257 $[433–176+H]^+$ (loss of one glucuronide moiety from m/z 433) as the major product ion in the MS^2 spectrum of molecular ion m/z 433 $[M+H]^+$ (Fig. 3(A)). The MS^3 spectrum of product ion m/z 257 $[M+H]^+$ (MS^3: m/z 257/433) was identical to the MS^2 spectrum of the authentic pterostilbene (Figs. 3(A) and 4(A)), indicating that peak 2 is the glucuronide metabolite of pterostilbene. The presence of the glucuronide metabolite of pterostilbene was also confirmed by the observation that peak 2 disappeared and one new peak (peak 1 at 21.27 min) was shown in the LC chromatogram of urine after treatment with β-glucuronidase and sulfatase (Fig. 2(B)). Peak 1 and authentic pterostilbene had the same molecular ions (m/z 257 $[M+H]^+$) and almost identical retention time (RT) and MS/MS spectrum, suggesting that peak 1 was pterostilbene (Figs. 4(A) and 4(B)).

Under negative ESI-MS detection, peak 2 was shown as one of the major peaks in the LC chromatogram of urine before treatment with β-glucuronidase and sulfatase (Fig. 2(C)). Peak 2 had a molecular ion m/z 431 $[M–H]^-$ (255 + 176), further suggesting that this peak was the glucuronide metabolite of pterostilbene (m/z 256). This was also confirmed by observing m/z 255 $[431–176–H]^-$ as one of the major product ions in the MS^2 spectrum of the molecular ion m/z 431 $[M–H]^-$ (Fig. 5(A)). In addition, the MS^3 spectrum of product ion m/z 255 $[M–H]^-$ (MS^3: m/z 255/431) was identical to the MS^2 spectrum of authentic pterostilbene (Figs. 5(A) and 5(C)). All of these features suggest that peak 2 was pterostilbene glucuronide. Since pterostilbene has only one hydroxyl group at position 4′, peak 2 was identified as pterostilbene 4′-glucuronide (Fig. 1).

The sulfate metabolite of pterostilbene could not be detected under APCI-MS detection. Peak 3 (pterostilbene sulfate) has the molecular ion m/z 257 $[M+H]^+$ (instead of the expected molecular ion m/z 337 $[M+H]^+$), which was the ion that lost the sulfate group $[337–80]^+$, under positive APCI-MS detection. Fortunately, negative ESI-MS detection could provide the molecular ion for pterostilbene sulfate (peak 3 at 31.19 min, m/z 335 $[M–H]^-$ (255 + 80)) (Fig. 2(C)). In SIM mode for pterostilbene sulfate (m/z 335 $[M–H]^-$ (255 + 80)), there was one major peak (peak 3, RT: 31.19 min) that had m/z

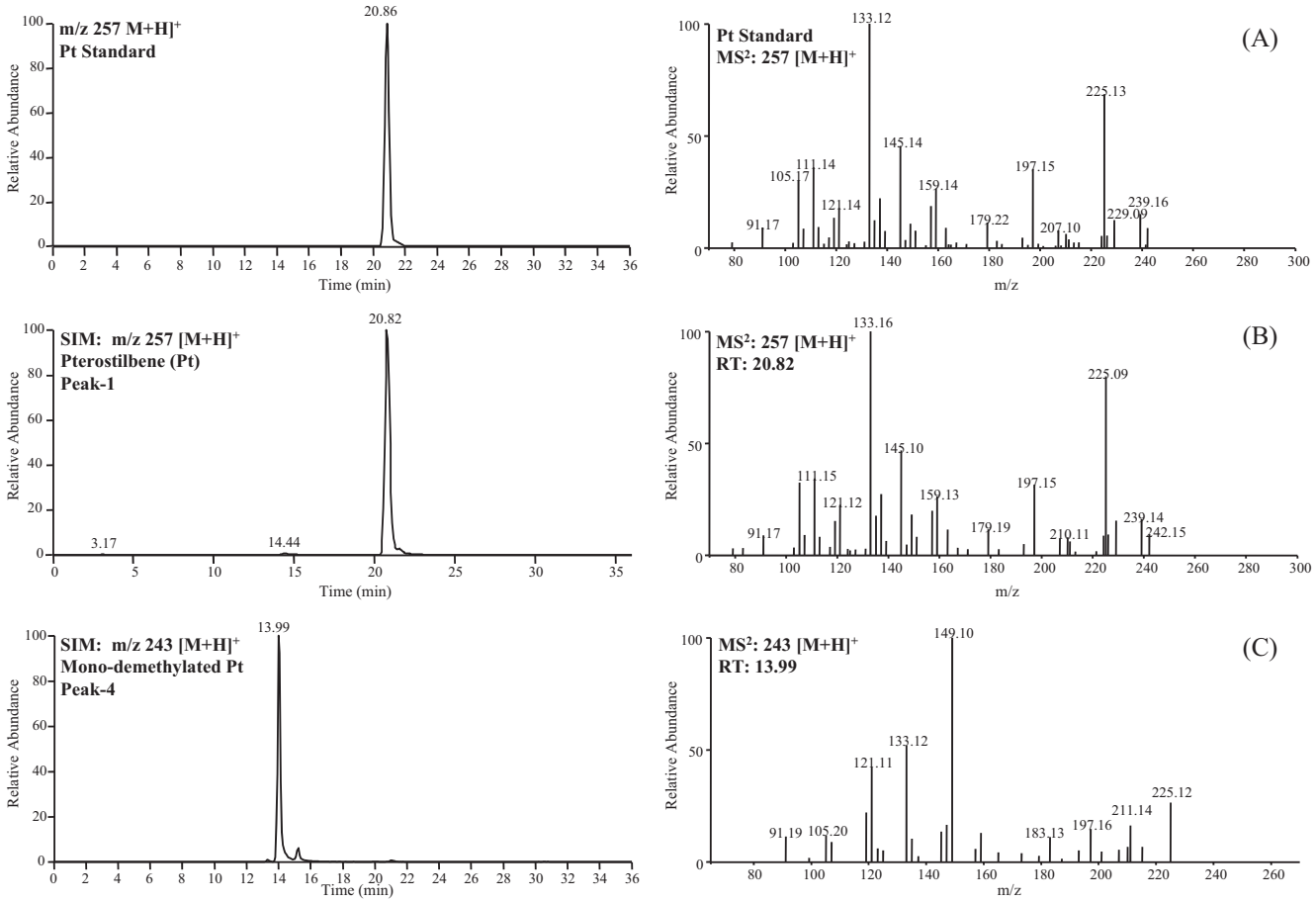

Figure 4. APCI-MS^2 (positive ion) spectrum of (A) pterostilbene standard and LC/APCI-MS^2 (positive ion) spectra of (B) pterostilbene (peak 1 in Fig. 2(B)) and (C) mono-demethylated pterostilbene (peak 4 in Fig. 2(B)). Pt stands for pterostilbene.

DOI: 10.1002/rcm

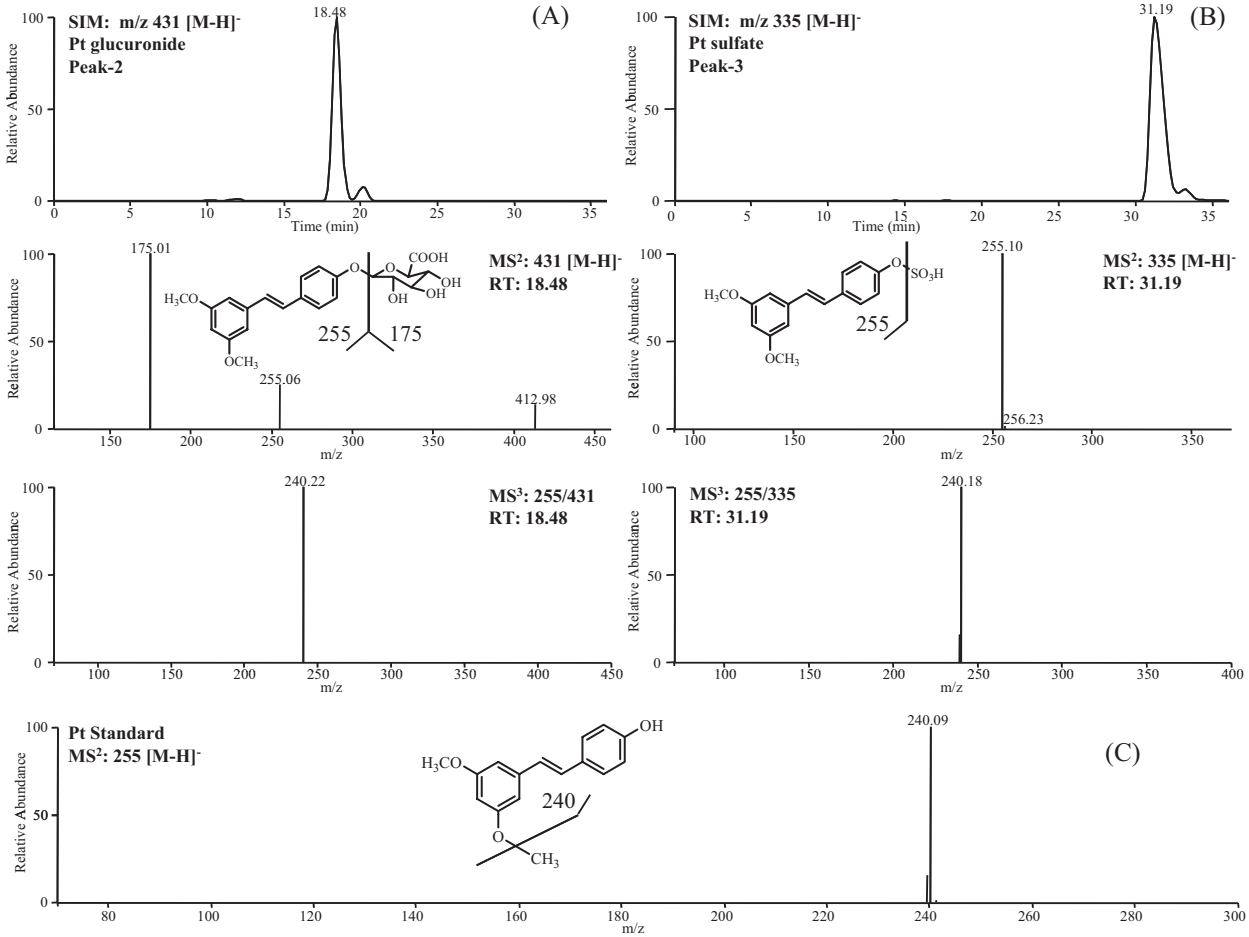

Figure 5. LC/ESI-MS^2 and -MS^3 (negative ion) spectra of (A) pterostilbene glucuronide (peak 2 in Fig. 2(C)) and (B) pterostilbene sulfate (peak 3 in Fig. 2(C)), and MS^2 spectrum of (C) pterostilbene standard. Pt stands for pterostilbene.

255 $[M–H]^-$ as the base product ion (Fig. 5(B)). The MS^3 spectrum of the product ion *m/z* 255 $[M–H]^-$ (MS^3: *m/z* 255/335) was identical to the MS^2 spectrum of authentic pterostilbene (Figs. 5(B) and 5(C)), further suggesting that peak 3 was pterostilbene sulfate. The presence of sulfate metabolites was also confirmed by the observation that peak 3 disappeared in the LC chromatogram of urine after treatment with β-glucuronidase and sulfatase (Fig. 2(D)). Similar to the glucuronide metabolite, we identified peak 3 as pterostilbene 4′-sulfate since pterostilbene has only one hydroxyl group at the 4′ position (Fig. 1).

Identification of the conjugated metabolites of mono-demethylated pterostilbene

Mono-demethylated pterostilbene glucuronide and mono-demethylated pterostilbene sulfate were identified as the major conjugated metabolites of mono-demethylated pterostilbene using LC/APCI- and LC/ESI-MS/MS. In the LC chromatogram obtained from APCI-MS detection (Fig. 2(A)), there was one major peak (peak 5 at 12.95 min) with molecular ion *m/z* 419 $[M + H]^+$ (243 + 176), indicating that this peak was the glucuronide metabolite of mono-demethylated pterostilbene. This was further confirmed by observing *m/z* 243 $[419–176 + H]^+$ (loss of one glucuronide moiety from *m/z* 419) as one of the major product ions in the MS^2 spectrum of molecular ion *m/z* 419 $[M + H]^+$ (Fig. 3(B)). The presence of glucuronide metabolites was also confirmed by the observation that peak 5 disappeared and one new peak (peak 4 at 14.02 min) was shown in the LC chromatogram of urine after treatment with β-glucuronidase and sulfatase (Fig. 2(B)). Peak 4 had a molecular ion *m/z* 243 $[M + H]^+$, which was 14 mass units less than the molecular ion of pterostilbene (*m/z* 257 $[M + H]^+$), suggesting that peak 4 was mono-demethylated pterostilbene. The MS^2 spectrum of peak 4 was identical to the MS^3 spectrum of the product ion *m/z* 243 $[M + H]^+$ of peak 5 (MS^3: *m/z* 243/419) (Figs. 3(B) and 4(C)), which further confirmed that peak 5 was the mono-glucuronide metabolite of mono-demethylated pterostilbene.

Under negative ESI-MS detection, peak 5 had molecular ion *m/z* 417 $[M-H]^-$ (241 + 176) (Fig. 2(C)), further suggesting that this peak was the glucuronide metabolite of mono-demethylated pterostilbene (*m/z* 242). This was also confirmed by observing *m/z* 241 $[417–176–H]^-$ as one of the major product ions in the MS^2 spectrum of molecular ion *m/z* 417 $[M–H]^-$ (Fig. 6(A)). In addition, the MS^3 spectrum of product ion *m/z* 241 $[M–H]^-$ (MS^3: *m/z* 241/417) was almost identical to the MS^2 spectrum of peak 4 (Figs. 6(A) and 6(C)). Therefore, peak 5 was identified as the mono-demethylated pterostilbene mono-glucuronide. We observed only one glucuronide metabolite of the mono-demethylated pteros-

DOI: 10.1002/rcm

RCM

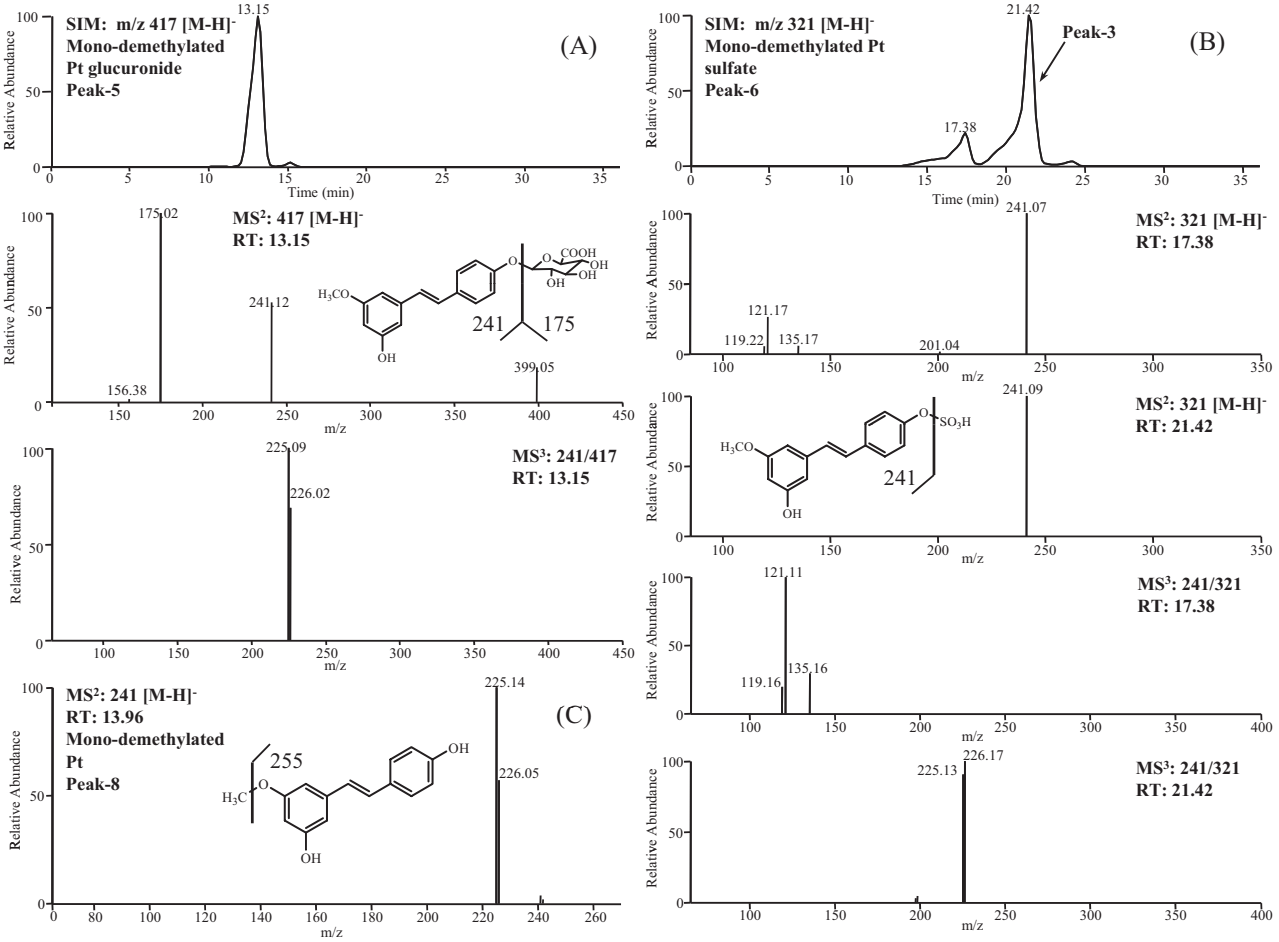

Figure 6. LC/ESI-MS^2 and -MS^3 (negative ion) spectra of (A) mono-demethylated pterostilbene glucuronide (peak 5 in Fig. 2(C)) and (B) mono-demethylated pterostilbene sulfate (peak 6 in Fig. 2(C)), and MS^2 spectrum of (C) mono-demethylated pterostilbene (peak 4 in Fig. 2(D)). Pt stands for pterostilbene.

tilbene even though it has two hydroxyl groups. The mono-glucuronide metabolite can be generated from the glucuronidation of mono-demethylated pterostilbene and/or the demethylation of pterostilbene 4′-glucuronide. Therefore, we tentatively identify it as shown in Fig. 1.

The sulfate metabolites of mono-demethylated pterostilbene could not be detected under APCI-MS detection. However, negative ESI-MS detection provided the molecular ions for mono-demethylated pterostilbene sulfate (peak 6 at 21.51 min, *m/z* 321 $[M–H]^-$ (241 + 80)). In SIM mode for mono-demethylated pterostilbene sulfate (*m/z* 321 $[M–H]^-$ (241 + 80)) there were two peaks that had *m/z* 241 $[M–H]^-$ as the base product ion. In order to further confirm that those compounds were the metabolites of mono-demethylated pterostilbene, we compared the MS^3 spectra of product ion *m/z* 241 $[M–H]^-$ of those two peaks with the MS^2 spectrum of mono-demethylated pterostilbene (peak 4 in Fig. 2(D)) obtained from urine samples after enzymatic hydrolysis (Figs. 6(B) and 6(C)). We found that only the peak at 21.42 min (peak 6) had a similar fragment ion mass spectrum as that of mono-demethylated pterostilbene (Figs. 6(B) and 6(C)). The MS/MS spectrum of the product ion *m/z* 241 $[M–H]^-$ of the peak at 17.38 min was completely different from the MS^2 spectrum of mono-demethylated pterostilbene (Figs. 6(B) and 6(C)), indicating that this peak was not the sulfate metabolite of mono-demethylated pterostilbene, even though it had almost identical MS^2 spectra as those of the sulfate metabolite of mono-demethylated pterostilbene. In addition, this metabolite was also observed in the urine sample obtained from mice in the control group. The peak observed in the control sample has identical MS^2 (*m/z* 321) and MS^3 (*m/z* 241/321) spectra as those of the peak at RT 17.38 min in the pterostilbene-treated sample (data not shown). Therefore, this metabolite is an endogenous metabolite instead of a metabolite of pterostilbene. This observation supports the conclusion that structural elucidation of conjugated metabolites cannot simply reply on the MS^2 spectrum, which has been widely used as the major tool for predicting the structures of the conjugated metabolites of dietary polyphenols in the literature. The presence of sulfate metabolites was also confirmed by the observation that peak 6 disappeared in the LC chromatogram of urine after treatment with sulfatase (Fig. 2(D)). Similar to the glucuronide metabolites, we also observed only one sulfate metabolite of the mono-demethylated pterostilbene even though it has two hydroxyl groups. The mono-sulfate metabolite can be generated from the sulfation of mono-demethylated pterostilbene and/or the demethylation of

DOI: 10.1002/rcm

pterostilbene 4′-sulfate. Therefore, we tentatively identified the mono-sulfate metabolite of mono-demethylated pterostilbene (peak 6) as shown in Fig. 1.

Identification of the conjugated metabolites of mono-hydroxylated pterostilbene

Since hydroxylation is considered to be one of the major phase I biotransformations of resveratrol in human liver microsomes, we also investigated the mono-hydroxylated pterostilbene and its conjugated metabolites. Three conjugated metabolites were identified in our study: mono-glucuronide, mono-sulfate, and glucuronide sulfate metabolites of mono-hydroxylated pterostilbene. Three major peaks were observed in the LC chromatogram under ESI-MS detection (Fig. 2(C)). They were marked as peak 8 (RT: 12.32 min) with the molecular ion m/z 447 $[M–H]^-$ (271 + 176), peak 9 (RT: 31.36 min) with the molecular ion m/z 351 $[M–H]^-$ (271 + 80) and peak 10 (RT: 27.49 min) with the molecular ion m/z 527 $[M–H]^-$ (271 + 176 + 80), suggesting that they were mono-glucuronide, mono-sulfate, and glucuronide and sulfate metabolites of mono-hydroxylated pterostilbene, respectively.

The existence of the mono-glucuronide metabolite was further confirmed by observing m/z 271 [448–176–H]$^-$ (loss of one glucuronide moiety from m/z 448) and m/z 175 $[M–H]^-$ (glucuronide moiety) as two of the major product ions in the MS^2 spectrum of molecular ion m/z 447 $[M + H]^+$ (Fig. 7(B)). The observation that peak 8 disappeared and one new peak (peak 7 at 17.44 min) was shown in the LC chromatogram of urine after treatment with β-glucuronidase and sulfatase (Fig. 2(D)) also confirmed the presence of glucuronide metabolites. Peak 7 had molecular ion m/z 271 $[M–H]^-$, which was 16 mass units higher than that of pterostilbene (m/z 255 $[M-H]^-$), suggesting that it was mono-hydroxylated pterostilbene. We also observed m/z 255 (271 – 16) as the major product ion in the MS^2 spectrum of peak 7. Moreover, the MS^3 spectrum of product ion m/z 255 $[M–H]^-$ of peak 7 (MS^3: m/z 255/271) was identical to the MS^2 spectrum of authentic pterostilbene (Figs. 5(C) and 7(A)). All these features suggested that peak 7 was mono-hydroxylated pterostilbene. The MS^2 spectrum of peak 7 was identical to the MS^3 spectrum of the product ion m/z 271 $[M–H]^-$ of peak 8 (MS^3: m/z 271/447) (Figs. 7(A) and 7(B)), which further confirmed that peak 8 was the mono-glucuronide metabolite of mono-hydroxylated pterostilbene. We observed only one glucuronide metabolite of mono-hydroxylated pterostilbene even though it has two hydroxyl groups. The mono-glucuronide metabolite can be generated from the glucuronidation of mono-hydroxylated pterostilbene and/or the hydroxylation of pterostilbene 4′-glucuronide. Therefore, we tentatively identify it as shown in Fig. 1.

The sulfate metabolite of mono-hydroxylated pterostilbene was confirmed by observing m/z 271 [352–80–H]$^-$ (loss

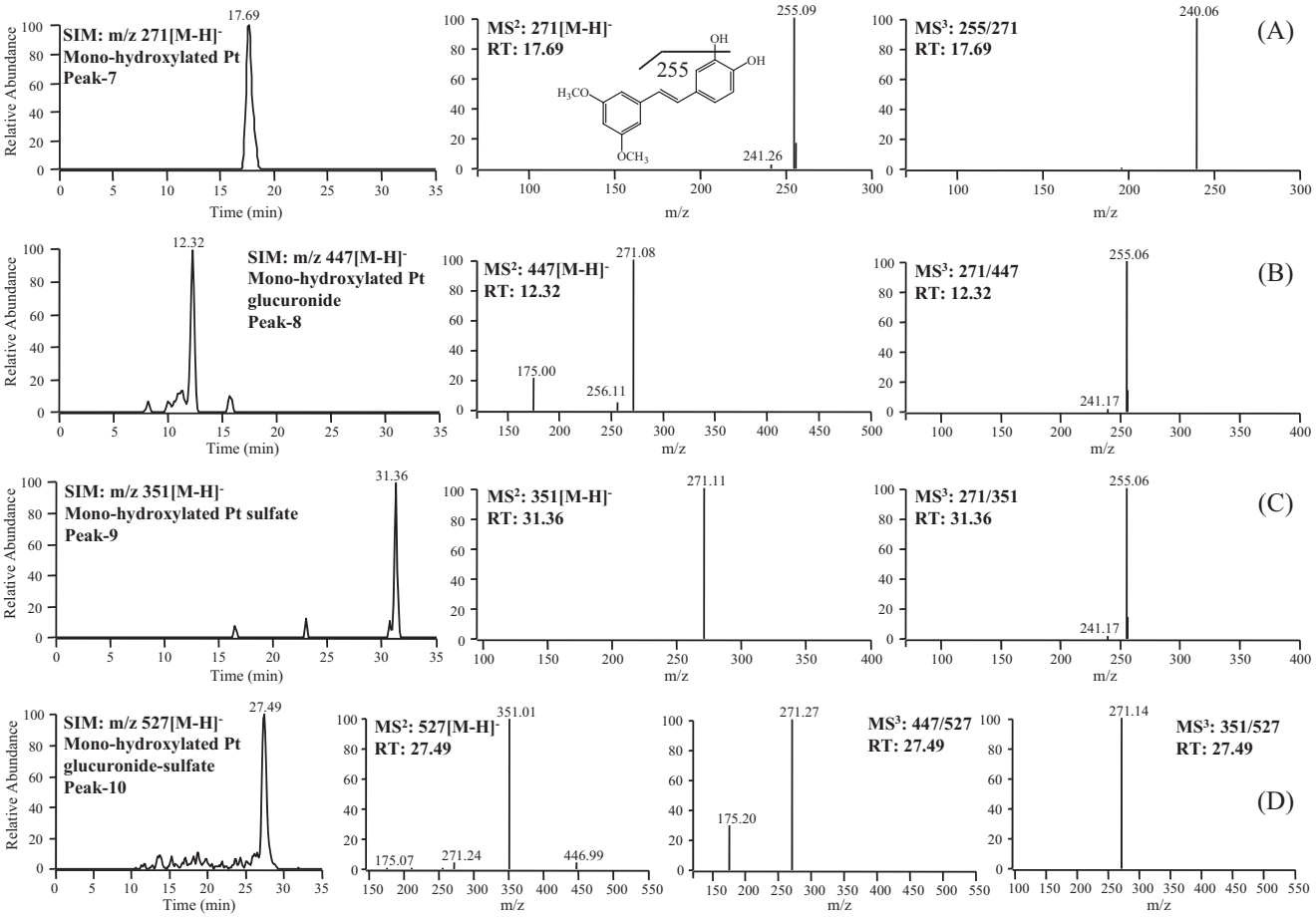

Figure 7. LC/ESI-MS^2 and -MS^3 (negative ion) spectra of (A) mono-hydroxylated pterostilbene glucuronide (peak 7 in Fig. 2(D)), (B) mono-hydroxylated pterostilbene glucuronide (peak 8 in Fig. 2(C)), (C) mono-hydroxylated pterostilbene sulfate (peak 9 in Fig. 2(C)), and (D) mono-hydroxylated pterostilbene glucuronide sulfate (peak 10 in Fig. 2(C)).

DOI: 10.1002/rcm

of one sulfate moiety from *m/z* 352) as one of the major product ions in the MS^2 spectrum of molecular ion *m/z* 351 $[M–H]^-$ (Fig. 7(C)). Even our chromatography method did not give us good separation of the sulfate metabolites of pterostilbene and mono-hydroxylated pterostilbene. The disappearance of peak 9 was observed in the LC chromatogram of urine after treatment with β-glucuronidase and sulfatase (Fig. 2(D)). In addition, the MS^3 spectrum of product ion *m/z* 271 $[M–H]^-$ of peak 9 (MS^3: *m/z* 271/351) was identical to the MS^2 spectrum of peak 7 (Figs. 7(A) and 7(C)), which confirmed that peak 9 was the mono-sulfate metabolite of mono-hydroxylated pterostilbene. Similar to the mono-glucuronide metabolite, we observed only one sulfate metabolite of the mono-hydroxylated pterostilbene. The mono-sulfate metabolite can be generated from the sulfation of mono-hydroxylated pterostilbene and/or the hydroxylation of pterostilbene 4′-sulfate. Therefore, we tentatively identify it as shown in Fig. 1.

In SIM mode with negative ESI-MS detection, we observed one peak corresponding to molecular ion *m/z* 527 $[M–H]^-$ (271 + 176 + 80) (peak 10 at 27.49 min, Fig. 7(D)). The MS^2 spectrum of peak 10 had product ions *m/z* 447 (loss of one sulfate moiety from *m/z* 527), *m/z* 351 (loss of one glucuronide moiety from *m/z* 527), *m/z* 271 (loss of one glucuronide moiety and one sulfate moiety from *m/z* 527), and *m/z* 175 (glucuronide moiety). All these features suggested that peak 10 was the glucuronide sulfate metabolite of mono-hydroxylated pterostilbene. In addition, the MS^3 spectrum of the product ion *m/z* 447 $[M–H]^-$ (MS^3: *m/z* 447/527) was almost identical to the MS^2 spectrum of mono-hydroxylated pterostilbene glucuronide (peak 8: *m/z* 447 $[M–H]^-$) and the MS^3 spectrum of product ion *m/z* 351 $[M–H]^-$ (MS^3: *m/z* 351/527) was almost identical to the MS^2 spectrum of mono-hydroxylated pterostilbene sulfate (peak 9: *m/z* 351 $[M–H]^-$) (Fig. 7(D)). All of these features suggested that that peak 10 was the glucuronide sulfate metabolite of mono-hydroxylated pterostilbene. The disappearance of peak 10 was observed in the LC chromatogram of urine after treatment with β-glucuronidase and sulfatase (Fig. 2(D)) further supported our conclusion that peak 10 was the glucuronide sulfate metabolite of mono-hydroxylated pterostilbene. This metabolite can be generated by further sulfation of the mono-hydroxylated pterostilbene glucuronide (peak 8) or by further glucuronidation of the mono-hydroxylated pterostilbene sulfate (peak 9) (Fig. 1). Since we only observed one peak, we tentatively identify it as shown in Fig. 1.

CONCLUSIONS

In this study, using both LC/APCI-MS/MS and LC/ESI-MS/MS analysis we successfully identified nine novel metabolites of pterostilbene from mouse urine samples collected 24 h after administration of 200 mg/kg pterostilbene through oral gavage (Fig. 1 and Table 1). To our knowledge, this is the first study to establish the mouse urinary metabolic profile of pterostilbene using multi-stage tandem mass spectrometry. Our results clearly indicate that pterostilbene can be metabolized in mice to generate the mono-demethylated and mono-hydroxylated metabolites. Pterostilbene and its mono-demethylated and mono-hydroxylated metabolites are good substrates for glucuronidation and sulfation to form related phase II metabolites.

It has been reported that resveratrol is extensively metabolized *in vivo* to generate the glucuronide and sulfate metabolites which are predominantly circulated in plasma and distributed to various tissues. Similarly, we found that glucuronide and sulfate metabolites are also the major metabolites of pterostilbene in mice. A possible metabolism pathway is established based on our observations and the literature reports on the biotransformation of resveratrol (Fig. 1). It is worthwhile to further study the pharmacokinetics of pterostilbene and the tissue distribution of pterostilbene and its major metabolites. Whether the newly identified mono-demethylated, mono-hydroxylated, glucuronide, and sulfate metabolites of pterostilbene are bioactive remains to be determined. The results would help us assess the relative contribution of pterostilbene metabolites to the disease preventive effects of pterostilbene.

SUPPORTING INFORMATION

Additional supporting information may be found in the online version of this article.

REFERENCES

1. Langcake P, Cornford CA, Pryce RJ. *Phytochemistry* 1979; **18**: 1027.
2. Maurya R, Ray AB, Duah FK, Slatkin DJ, Schiff PL. *J. Nat. Prod.* 1984; **47**: 179.
3. Sehadri R. *Phytochemistry.* 1972; **11**: 881.
4. Paul B, Masih I, Deopujari J, Charpentier C. *J Ethnopharmacol.* 1999; **68**: 71.
5. Cichocki M, Paluszczak J, Szaefer H, Piechowiak A, Rimando AM, Baer-Dubowska W. *Mol. Nutr. Food Res.* 2008; **52** (Suppl 1): S62.
6. Suh N, Paul S, Hao X, Simi B, Xiao H, Rimando AM, Reddy BS. *Clin. Cancer Res.* 2007; **13**: 350.
7. Pari L, Satheesh MA. *Life Sci.* 2006; **79**: 641.
8. Rimando AM, Cuendet M, Desmarchelier C, Mehta RG, Pezzuto JM, Duke SO. *J. Agric. Food Chem.* 2002; **50**: 3453.
9. Manickam M, Ramanathan M, Jahromi MA, Chansouria JP, Ray AB. *J. Nat. Prod.* 1997; **60**: 609.
10. Remsberg CM, Yanez JA, Ohgami Y, Vega-Villa KR, Rimando AM, Davies NM. *Phytother. Res.* 2008; **22**: 169.
11. Lambert JD, Sang S, Hong J, Kwon SJ, Lee MJ, Ho CT, Yang CS. *Drug Metab. Dispos.* 2006; **34**: 2111.
12. Baur JA, Sinclair DA. *Nat. Rev. Drug Discov.* 2006; **5**: 493.
13. Li S, Wang Z, Sang S, Huang MT, Ho CT. *Mol. Nutr. Food Res.* 2006; **50**: 291.
14. Steenwyk RC, Tan B. *Xenobiotica* 2010; **40**: 62.

DOI: 10.1002/rcm